Available online at www.sciencedirect.com
SCIENCE DIRECT
Journal of Catalysis 227 (2004) 459–469
JOURNAL OF CATALYSIS
www.elsevier.com/locate/jcat

A rational design of alkyl-aromatics dealkylation–transalkylation catalysts using C_8 and C_9 alkyl-aromatics as reactants

José M. Serra [a], Emmanuelle Guillon [b], Avelino Corma [a,*]

[a] *Instituto de Tecnología Química, UPV-CSIC, Av. de los Naranjos s/n, 46022 Valencia, Spain*
[b] *Institut Français du Pétrole, CEDI René Navarre. BP 3, 69390 Vernaison, France*

Received 3 June 2004; revised 29 July 2004; accepted 6 August 2004

Available online 17 September 2004

Abstract

A catalyst has been designed to optimize the dealkylation of ethyl and propyl aromatics while producing the transalkylation of tri- and tetramethylbenzene with toluene in order to maximize xylenes and benzene when processing heavy reformate. Conversion of model ethyl-aromatics under realistic transalkylation conditions has been studied over two reference catalysts and seven different acid zeolites including topologies with channel systems containing 10 MR, 12 MR, and 10 + 12 MR. Catalytic testing was accomplished by means of a high-throughput reactor system. It has been found that zeolite structure has a direct influence on the ethyl dealkylation/transalkylation activity, increasing the ethylbenzene conversion and dealkylation selectivity when decreasing the zeolite pore volume. Moreover, Re/IM-5 and, specially, Re/ZSM-5 zeolites show an excellent dealkylation activity. Ethylbenzene undergoes different bimolecular reactions giving as primary products either benzene and diethylbenzene or toluene and ethyltoluene, each reaction involving a different biphenylic intermediate and the selectivity toward each mechanism is directly influenced by the zeolite pore size and geometry.

Keywords: Ethylbenzene; Transalkylation; Dealkylation; Zeolites; Heavy reformate

1. Introduction

Aromatics are an important raw material for the production of monomer for polyesters and phthalates, engineering plastics, detergents, pharmaceuticals, etc. Among them, ethylbenzene, and benzene, toluene, and xylenes (BTX) are the three basic aromatic starting reactants.

Catalytic reforming of naphtha and naphtha pyrolysis are the main sources of BTX. The yields obtained from the above processes are normally controlled by thermodynamics, and this produces a substantial mismatch between the supply and the market demand [1] for the different aromatics. Indeed, toluene which has the lowest market demand always comes in surplus from the reformate and gasoline pyrolysis, whereas benzene and xylenes, which are produced in lower amounts, are in strongly growing demand. Thus, different industrial processes (Xylene-Plus [2,3], Tatoray [4,5], and TransPlus [6]) transalkylate toluene with less valuable C_9^+ aromatics derived from heavy reformate stream, to produce preferentially xylenes. Heavy reformate contains not only poly-methyl-aromatics like trimethylbenzene and tetramethylbenzene, useful for producing xylenes directly by transalkylation with toluene, but also ethyl- and propyl-aromatics, that can yield undesired heavy C_{11}^+ alkyl-aromatics during the process. Therefore, an optimized transalkylation process designed to maximize xylenes will involve transalkylation of methyl groups and dealkylation of ethyl and propyl groups.

Transalkylation of alkyl-aromatics is carried out using acid zeolites as catalysts under hydrogen pressure. For this process it would be highly desirable to develop tailor-made catalysts with improved methyl-transalkylation activity, while giving ethyl and propyl dealkylation. This type of catalysts not only will improve the yields of benzene

* Corresponding author. Fax: +34 96 3877809.
E-mail address: acorma@itq.upv.es (A. Corma).

0021-9517/$ – see front matter
doi:10.1016/j.jcat.2004.08.006

and xylenes but also the catalyst life [7,8] by decreasing the yield of A_{10}^+ and A_{11}^+ products that can produce coke which will result in pore blocking. Therefore, a successful dealkylation–transalkylation catalyst should accomplish the following specific functions:

(i) Capable of processing feeds with high contents of heavy reformate;
(ii) Avoid the formation of undesirable A_{10}^+ products from disproportionation of A_9^+ products;
(iii) Selective dealkylation of A_9 and A_{10} reactants and specially deethylation of ethyltoluenes and ethylxylenes that represent about 40 wt% of heavy reformate;
(iv) Avoid the formation of naphthenes and paraffins from hydrogenation of aromatic rings and cracking.

In the present work, the mechanism of different reactions occurring during the dealkylation–transalkylation of ethylbenzene has been studied. Taking into account the characteristics of the transition states for the different reactions, it is predicted that molecular sieve catalysts with medium and large pores within the same structure should be more adequate than the actual large-pore molecular sieves used in industry. This has been proven by studying a series of molecular sieve structures with medium, large, and medium plus large pores, together with two reference catalysts.

2. Experimental

2.1. Catalyst preparation

Beta, mordenite, and ZSM-5 zeolites were commercial samples supplied by PQ (CP811, CBV30A, and CBV3020 products). Zeolite NU-87, IM-5, mazzite, and ITQ-23 samples were synthesized in our laboratory following the procedures reported in [9–12].

Na zeolites were converted into the acid form by ion exchange with ammonium chloride for 2 h at 80 °C and ulterior calcination at 580 °C for 5 h. The acid samples were impregnated with an aqueous solution of perrhenic acid (Acros Organics, 76.5%), dried at 100 °C overnight, calcined at 500 °C for 2 h, and pelletized. Finally, they were reduced in hydrogen flow at 450 °C for 1 h in the same catalytic testing rig. Reference catalysts were prepared by IFP. The characteristics of the two reference catalysts composed of dealuminated mordenite, an amorphous binder, and a metallic component (Ni or Re) are given in Table 1.

Table 1
Composition of three transalkylation industrial catalysts used as reference

Catalyst	Zeolite	Metal	Preparation	Binder
Ni/MOR	Mordenite	Ni (1%)	Ion exchange	20% γ-Al_2O_3
Re/MOR	Mordenite	Re (0.3%)	Impregnation	30% γ-Al_2O_3

2.2. Characterization

A Nicolet 710 FTIR spectrometer was used to follow the pyridine adsorbed on the acid sites. For doing this, self-supported wafers with 10 mg/cm^2 were pretreated overnight under vacuum at 673 K and cooled down to room temperature. After acquisition of the spectrum in the OH stretching region, pyridine vapor (6.6 kPa) was admitted to the cell until equilibrium was reached. The samples were then desorbed under vacuum (10^{-3} mbar) at 250 and 350 °C with spectra acquisition at room temperature after each desorption treatment. All the spectra were scaled according to the sample weight. Absorption coefficients calculated by Emeis [14] were used. The pore volume and microporous surface area of the samples were obtained with an ASAP 2000 apparatus. Calculations were performed following the method developed by De Boer et al. [13] using the N_2 absorption isotherms at 77 K.

A 2910 Micromeritics system was used to carry out temperature-programmed reduction of metal incorporated catalysts. Thus, 100 mg of calcined sample was degassed under Ar flow for 1 h and then was subjected to reduction under H_2/Ar (1/9) flow, and heating rate of 10 °C/min till 850 °C. The H_2 consumption was measured by a TCD.

2.3. Catalytic studies

High-throughput testing was accomplished using a system [15,16] of 16 continuous fixed-bed parallel microreactors, able to work up to 80 bar and up to 700 °C (Spider reactor). Each reactor is fed and the flow measured independently by means of one liquid and one gas mass-flow controller, being possible to operate with this feeding system in a wide range of contact times and hydrogen to hydrocarbon ratios. The amount of catalyst can be varied from 50 to 1000 mg catalyst. Temperature and pressure were measured in each catalyst bed. The hydrocarbon used as model feed was ethylbenzene 99% (Fluka) and *p*-ethyltoluene 90% (Aldrich).

The simultaneous catalytic experiments were carried out at 25 bar total pressure, temperature 400 °C, hydrogen to hydrocarbon ratio of 8.5 mol mol^{-1}, and the WHSV was varied between 4 and 1400 h^{-1}. The amount of catalyst (particle size 0.4–0.6 mm) in each fixed-bed microreactor was 200 mg. Reaction products were analyzed on line by using a gas chromatograph (Varian 3800GC) equipped with a diphenyldimethylpolysiloxane capillary column. The duration of the experiments was longer than 10 h and the results given below were obtained for a TOS of 8 h. Dealkylation selectivity and transalkylation (to form diethylbenzene) selectivity were calculated considering the molar composition of the product stream:

$$S_{\text{Dealkylation}} = \frac{\%\text{Ethane}}{\%\text{Ethane} + \%\text{dEB}} \cdot (\%\text{Bz} + \%\text{Ethane} + \%\text{dEB}),$$

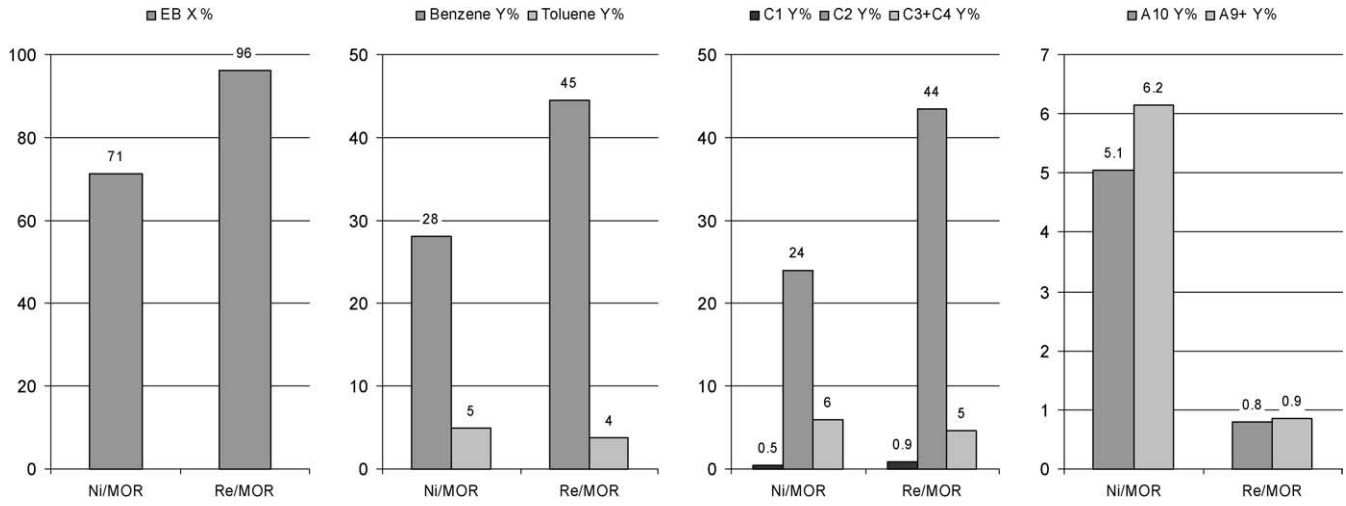

Fig. 1. Catalytic performance of two reference catalysts: EB conversion and molar yields. (Reaction conditions: 25 bar, 400 °C, WHSV 8 h^{-1}, and H_2/EB 8.5, TOS ~ 8 h.)

$$S_{\text{Transalkylation}} = \frac{\%\text{dEB}}{\%\text{Ethane} + \%\text{dEB}} \cdot (\%\text{Bz} + \%\text{Ethane} + \%\text{dEB}).$$

3. Results and discussion

3.1. Reference catalysts

Catalytic conversion of ethylbenzene (EB) with two reference catalysts supplied by IFP are displayed in Fig. 1. Both catalysts gave high levels of conversion, with the Re/mordenite the most active one. The major products obtained during the conversion of EB were benzene, ethane, and diethylbenzene, while toluene, ethyltoluene, xylenes, naphthenes, and cracking products (C_1, C_3, and C_4) were obtained in much lower amounts. Ethane yield can be used as a tracer for the ethyl-dealkylation reaction, while the yield of diethylbenzene (A_{10}) defines the ethyl-transalkylation activity, and benzene is a product formed in both reactions.

Olefins produced by dealkylation and acid cracking were totally and rapidly hydrogenated over both catalysts, since their presence was not detected in the reaction products. Then, dealkylation over acid Brønsted sites [17] should be followed by rapid olefin hydrogenation over adjacent metals sites, in order to reduce catalyst deactivation by olefin oligomerization and coke formation within the micropores. Therefore, a good dealkylation–transalkylation catalyst should have a good balance and proximity between acid sites and selective hydrogenation metal sites. Regarding the formation of other light alkanes, methane is detected in very low concentrations while propane and butanes are detected in higher concentrations (up to 5% molar yield). The selected content of rhenium allows minimization of the cracking and hydrogenation of aromatics but maintained the olefin hydrogenation activity and, then, the catalyst life. Indeed for 0.3 wt% content of Re 0.1 mol%, naphthenes (ethylcyclohexane and cyclohexane) were observed at 400 °C and WHSV 8 h^{-1}. The low yield of naphthenes observed with this Re catalyst can be due to a low activity of the metal for hydrogenation of the aromatic ring and/or to a cracking of the naphthenes formed by hydrogenation into $C_3 + C_4$ products (Scheme 1). The yields of $C_3 + C_4$ obtained with the Re-beta (6.8% at 50%X_{EB}) are slightly higher than those obtained with Re-free beta (4.5% at 50%X_{EB}). These results indicate that (0.3 wt%) Re has a low activity for aromatics hydrogenation under the reaction conditions given in this work. However, it must be said that if the amount of Re is increased to 1 wt%, then the amount of $C_3 + C_4$ strongly increases (12.2% at 50%X_{EB}) and methane is also formed (0.6%).

Re/mordenite catalyst exhibits the highest EB conversion (~ 95%) with a very high yield of ethane (~ 45%) (dealkylation) and benzene (~ 45%) while the yield to polyalkylbenzenes (diethylbenzene ~ 1%), cracking (5%), and toluene (4%) is low. The Ni/mordenite catalyst shows lower EB conversion and ethyl-dealkylation selectivity, with a higher selectivity to transalkylation products (dEB). Besides, after the stabilization of the reaction process using both catalysts, significant catalyst deactivation during the experiment (10 h) was not observed. In conclusion, the reference catalysts based on Re/mordenite presents the best EB dealky-

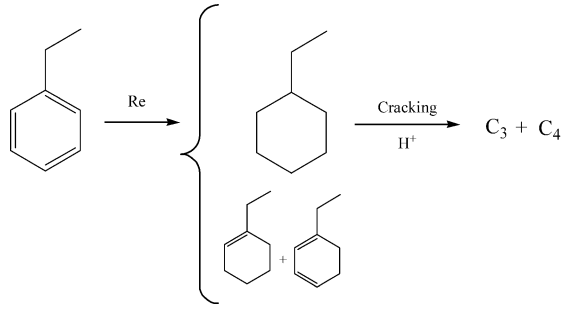

Scheme 1.

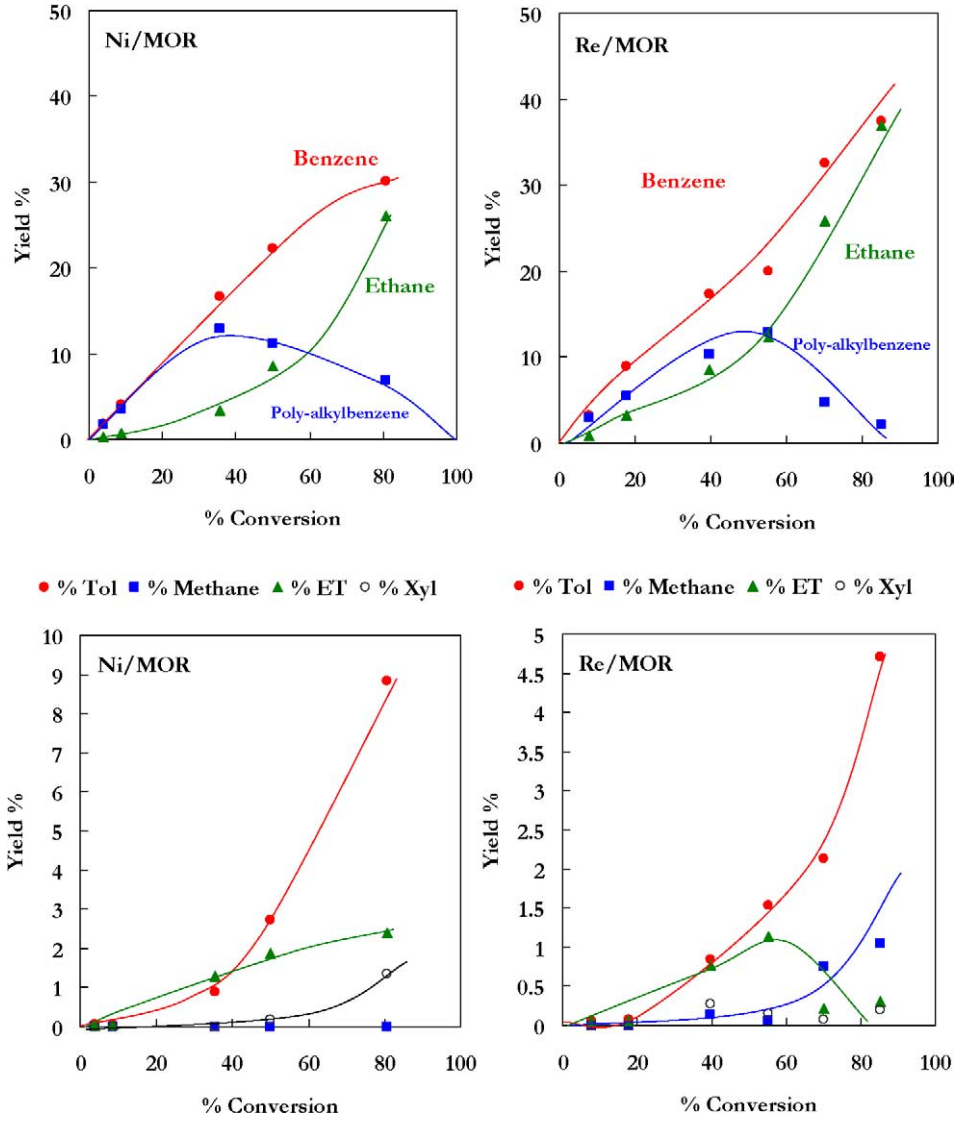

Fig. 2. Evolution of molar product yield with the EB conversion for two reference catalysts. (Reaction conditions: 25 bar, 400 °C, WHSV 4 to 1400 h^{-1}, and H_2/EB 8.5, TOS ∼ 8 h.)

lation performance under realistic reaction conditions, and will be used as a reference catalyst.

3.2. *Reaction mechanism*

From the results obtained up to now, it appears that a series of parallel and consecutive reactions occurs when reacting EB. Then, in order to discuss the reaction mechanisms, a detailed reaction network should be constructed. To do this and to find which products are primary, secondary, stable, or unstable, we need to consider the yields of products at different levels of conversion. Thus, the space velocity was varied in a wide range (4 to 1400 h^{-1}) achieving conversions from 5 to 90%. The yields of the different products versus total conversion are plotted in Fig. 2. At low EB conversions, the main products are poly-alkyl-aromatics, specially diethylbenzene (dEB), while the yield of ethane is lower than the dEB yield even for conversions in the order of 50%. Therefore, it can be said that the ethyl group dealkylation rate is lower than the transalkylation rate under these reaction conditions. At higher conversions (50%), the yield of poly-alkyl-aromatics goes through a maximum (10%) conversion, and then starts to decrease while the yield of ethane increases exponentially. This behavior can be explained considering that the complete dealkylation of poly-alkyl-aromatics produces, at least, two molecules of ethane per molecule converted. Scheme 2 shows a proposed reaction scheme for single dealkylation–transalkylation of ethyl groups, which constitute the principal reactions in the process.

The initial selectivities to different reaction products are displayed in Table 2. It can be seen there that depending on the catalyst the rate of ethyl-transalkylation is from two to seven times faster than the rate of ethyl dealkylation. During the initial reaction events, the EB mainly undergoes disproportionation yielding poly-alkylbenzenes. Therefore,

Table 2
Initial selectivities for the reference catalysts

	EB X%	Dealkylation	Transalkylation	$C_3 + C_4$	Toluene	ET	Xylenes	Naphtenes	Methane
Ni/MOR	3.9	11.1	84.5	0.84	3.5	0.72	0.0	0.0	0.0
Re/MOR	7.9	20.6	76.2	1.44	1.71	0.53	0.0	0.0	0.0

Reaction conditions: 25 bar, 400 °C, WHSV = 1400 h^{-1}, and H_2/EB ratio 8.5, TOS ∼ 8 h.

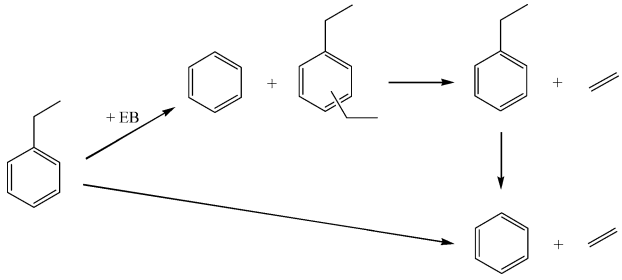

Scheme 2.

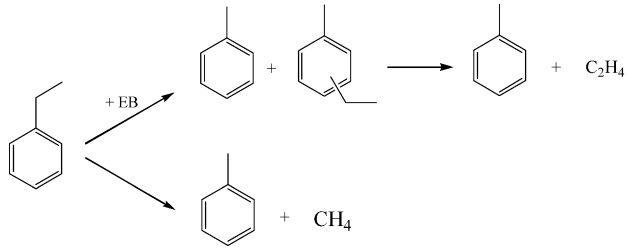

Scheme 3.

an improved catalyst for toluene/heavy reformate upgrading should reverse the relative order of activities observed above by increasing strongly the dealkylation, and avoiding the early formation of poly-alkylbenzenes that can produce catalyst deactivation by pore blocking and coke formation.

Fig. 2 shows also the evolution of minor products, i.e., toluene, ethyltoluene, methane, and xylenes, with EB conversion. It is remarkable the relatively high toluene (9%) yield obtained at high conversions (80%) with the Ni/mordenite catalyst. The formation of toluene from EB involves the cracking of the C–C bond of the ethyl group in the EB molecule. Two mechanisms can be proposed for explaining the formation of toluene from EB (Scheme 3): (i) the monomolecular cracking of the C–C bond of the ethyl group to yield toluene and methane and (ii) a bimolecular reaction, in which the terminal methyl is transferred from one EB molecule to another producing toluene and ethyltoluene through a biphenylic-type transition state (see Scheme 4). If the monomolecular mechanism will be the preferred one, then the ratio of the initial selectivities for methane and toluene should be close to one. However, as can be seen in Table 2, this is not the case, since methane is not detected as a primary product. On the other hand, if the main mechanism for toluene formation involves the bimolecular reaction depicted in Scheme 4, then the ratio of the initial selectivities for toluene and ethyltoluene should be one or higher than one depending if ethyltoluene does or does not dealkylate before diffusing out of the pores and desorbing into the gas stream. The results from Table 2 show that ethyltoluene is indeed formed as a primary product and the ratio of toluene to ethyltoluene when conversion tends to zero (initial selectivity) is higher than one, indicating that dealkylation of ethyltoluene has already occurred at those levels of conversion. Then, if we assume that the bimolecular mechanism (ii) is the only one responsible for formation of toluene and ethyltoluene at low levels of conversion, it is possible from the initial selectivities to calculate the fraction of ethyltoluene that has been dealkylated to produce toluene by means of Eq. (1). Considering the initial selectivities of Table 2, this ratio is 66 and 53% for Ni/mordenite and Re/mordenite, respectively, which is higher than the fraction of EB dealkylated.

$$\frac{ETOL_{\text{Dealkylated}}}{ETOL_{\text{Formed}}} = \frac{IS_{\text{Tol}} - IS_{\text{ETol}}}{IS_{\text{Tol}} + IS_{\text{ETol}}}. \tag{1}$$

From the above results, it is clear that dealkylation is faster for ET than for EB. In order to further check this, we have fed pure ET under the same reaction conditions, and the initial rate for dealkylation was 0.190 mol h^{-1} g_{cat}^{-1}, while for EB was 0.107 mol h^{-1} g_{cat}^{-1} using Re/mordenite-based catalysts. From these results, we can conclude that, indeed, the

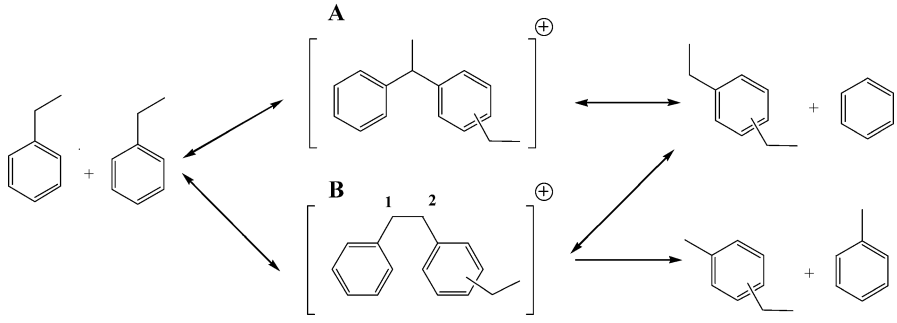

Scheme 4.

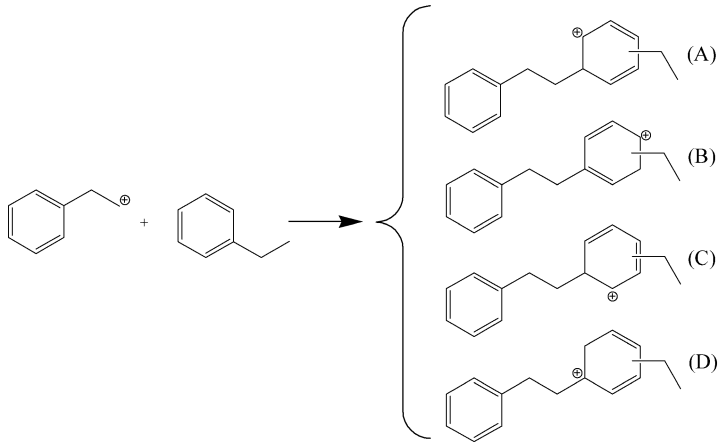

Scheme 5.

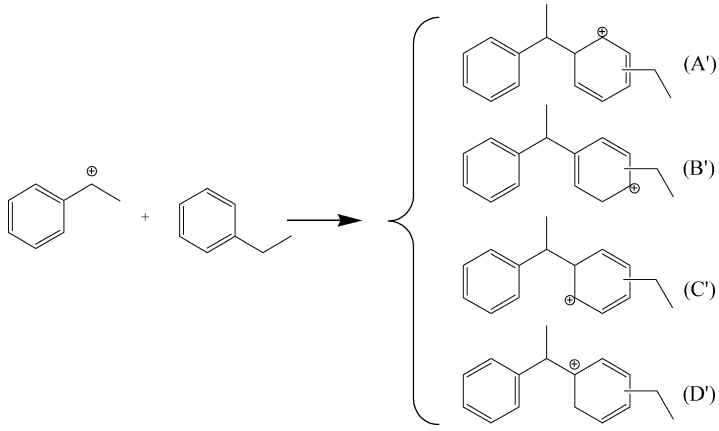

Scheme 6.

initial rate of dealkylation of ET is about two times higher than EB and consequently the bimolecular mechanisms (ii) is feasible. A mechanism of this type involves necessarily the formation of a "primary" carbocation that will perform an electrophilic attack to another molecule of EB, forming the possible intermediates shown in Scheme 5. β-Scission of intermediates A and C restores the reactants, while β-scission of D will produce toluene plus ET. We have said before that a successful catalyst for treating heavy naphtha reformate should favor dealkylation of the heavier alkyl-aromatics, instead of transalkylation, as was observed to occur with EB.

When comparing both reference catalysts, they show a similar behavior in ethyl dealkylation and transalkylation to form dEB. However, the Ni-MOR catalyst shows a little higher selectivity to toluene and ET. This selectivity toward toluene and ET formation through a bimolecular mechanism was reproduced using beta zeolite, and this can be explained by considering that nickel species inside the zeolite porous system contribute to the stabilization of transition states and/or directs the rupture of the biphenylic state in the adequate C–C bond (Schemes 4 and 5).

Table 2 also shows that the desired xylenes are not produced directly from EB under our reaction conditions, and they are detected in very low amounts (0.5 to 1%) even at high levels of conversion ($X = 80\%$). Thus, xylenes should be formed, under our reaction conditions, through the secondary disproportionation of toluene and not through the direct EB isomerization [18,19]. It is important to remark that these reference catalysts do not show a significant activity either for the aromatic ring hydrogenation or for methane formation (hydrogenolysis).

While alkyl-aromatic dealkylation is a monomolecular reaction, it is accepted [20] that transalkylation reactions require the close interaction between two alkyl-aromatic molecules. This, in a Langmuir–Hinshelwood formalism, implies that an adsorbed and activated molecule on an acid site reacts with another adsorbed molecule to yield a biphenylic intermediate [21–25] inside the zeolite channel system. More specifically, in the EB transalkylation to give benzene plus dEB, a secondary carbenium ion formed on the alkyl chain would be the alkylating agent to form a series of biphenylethane carbocations (Scheme 6). Among the different carbocations, the D′ is the most stable one and consequently its surface concentration should be higher. The β-scission of carbocation (A′) and (C′) restores the original reactants, while the β-scission of the most stable (D′) will yield benzene and dEB as final products. While this is what carbocation chemistry will predict, in the case of reactions

occurring in confined spaces, the type of biphenylic intermediate and the scission type will also be determined by the size and geometry of the intrazeolitic pores in which the reaction occurs. In any case, we should take into account that the size of the intermediates involved in transalkylation reactions are much larger than the one involved in dealkylation. Therefore, the zeolite pore topology should determine the selectivity to transalkylation versus dealkylation reactions by restricting the formation of bulkier transition states, something that has also been proposed previously for the alkylation of toluene [26] and isomerization of xylenes [27]. In the next part of the work, seven zeolites with different pore topologies including 10-, 12-, and 10 × 12-MR pores will be tested for EB conversion with the aim of determining the influence of the structure on: (i) activity ratio between ethyl transalkylation and dealkylation [28], and (ii) selectivity of the two transalkylation reactions showed above (Schemes 5 and 6).

3.3. Influence of zeolite structure

In Table 3 the composition, the BET surface area, and acidity of the seven Re zeolites used in this study are given. TPR experiments of the impregnated samples (Re 0.3%) showed a similar profile for all samples, with a single hydrogen consumption peak centered at 400 °C. Hence, rhenium is in reduced form under reaction conditions. This point was confirmed by XPS measurements (VG-Escalab 210) with a Re/beta sample reduced in situ at different temperatures.

Catalytic results at two levels of conversions are displayed in Table 4. A general trend can be observed from results presented in Tables 3 and 4. Regardless of the acidity measured by pyridine, the higher the pore diameter of the studied zeolites the lower the EB conversion. More specifically, four types of catalytic behavior can be distinguished depending on zeolite topology (values for WHSV 14 h^{-1}):

1. Zeolites ZSM-5 [29] and IM-5, with 10-MR pores, show high EB conversion (90%), very high dealkylation selectivity (90%), and a *very low transalkylation* selectivity.
2. Zeolite mordenite and mazzite, monodimensional 12-MR zeolites, show a lower EB conversion (75%) with high dealkylation selectivity (75%) and low transalkylation selectivity.
3. Zeolites NU-87 and ITQ-23, with intercrossing 10-MR and 12-MR pores, show a high conversion (85%) with medium dealkylation selectivity (50%) and medium transalkylation selectivity.
4. Beta, a tridimensional 12-MR pore zeolite, shows a medium EB conversion (75%) with low dealkylation selectivity (32%) and medium to high transalkylation selectivity.

These trends have been summarized in Figs. 3 and 4, where EB conversion and dealkylation selectivity for a representative zeolite of each group have been plotted. The most interesting aspect is that EB dealkylation activity increases when decreasing the zeolite pore size. The high dealkylation activity and selectivity shown by 10-MR zeolites, specially

Table 3
Composition and physicochemical characterization of zeolitic samples (0.3% Re)

Zeolite	Code	Channels	Micropore volume227/g)	$S_{\mu pore}$ (m^2/g)	Si/Al	Acidity (μmol pyr/gr)			
						Brønsted		Lewis	
						250 °C	350 °C	250 °C	350 °C
ZSM-5	MFI	10×10 MR	0.12	228	18	44	25	9	6
IM-5	–	10×10 MR *	0.13	300	15	29	17	7	6
Mazzite	MAZ	12 MR	0.14	310	14	45	27	9	9
Mordenite	MOR	12 MR	0.15	339	18	79	37	25	24
NU-87	NES	10×12 MR	0.16	331	16	70	48	26	24
ITQ-23	–	10×12×12 MR	0.18	370	15	49	29	37	31
Beta	BEA	12×12 MR	0.20	325	13	31	15	53	42

Table 4
Catalytic performance of six different zeolites: EB conversion and molar selectivity

	WHSV 14 h^{-1}					WHSV 4 h^{-1}				
	EB *X*%	Dealkylation	Transalkylation	Toluene	$C_3 + C_4$	EB *X*%	Dealkylation	Transalkylation	Toluene	$C_3 + C_4$
Beta	74.0	34.5	18.6	20.1	26.8	87.3	36.1	4.3	29.5	30.1
ITQ-23	85.3	53.0	2.8	24.5	19.7	97.4	45.3	0.8	29.6	24.3
NU-87	83.7	50.3	17.2	13.8	18.7	91.7	55.9	5.6	21.6	16.8
Mordenite	68.4	75.5	7.0	5.9	11.6	76.4	75.4	3.2	9.8	11.5
Mazzite	76.1	74.4	5.0	7.9	12.6	93.5	69.0	0.8	11.7	18.6
IM-5	93.1	89.4	1.3	2.1	7.2	95.4	83.1	0.8	3.2	12.9
ZSM-5	90.9	92.4	0.9	1.3	5.3	92.4	86.7	0.7	2.2	10.4

Reaction conditions: 25 bar, 400 °C, WHSV 4–14 h^{-1}, and H_2/EB 8.5, TOS ∼ 8 h.

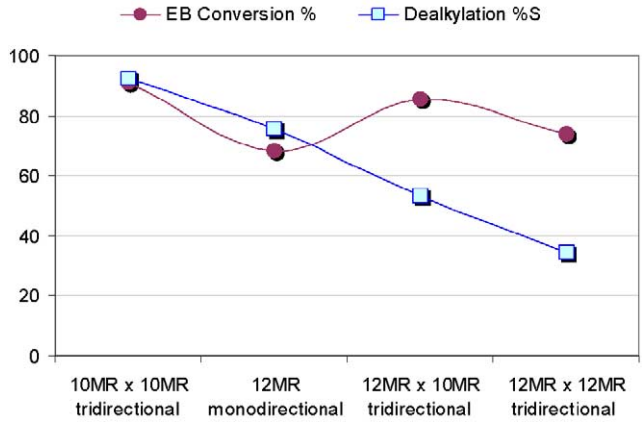

Fig. 3. Exemplified catalytic behaviors for different zeolite structures under industrial-practiced reaction conditions.

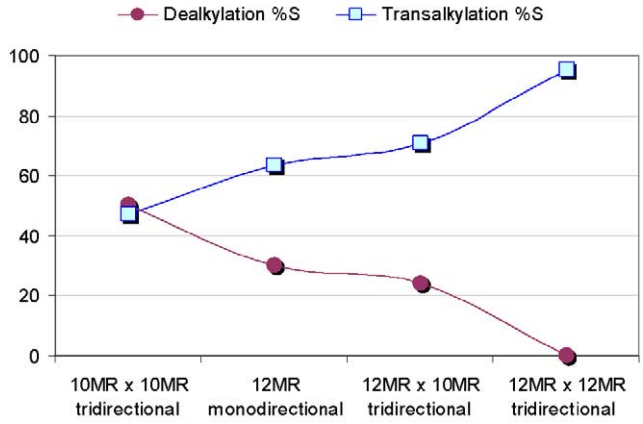

Fig. 4. Exemplified catalytic behaviors for different zeolite structures at high space velocities ($X \sim 5\%$, WHSV 1400 h^{-1}, TOS ~ 8 h).

ZSM-5, is not only due to the total number of acid sites, but can be related to the high confinement of the EB molecule within the pores. This restricts the competitive transalkylation reaction by avoiding the formation (Scheme 4) of bulky intermediates (~ 10.5 Å) and bulky final products like dEB, whose diffusion through 10-MR channels is hindered. This behavior is independent of the level of conversion (Fig. 6). This catalytic behavior observed above has been confirmed by using ethyltoluene as reactant under the same reaction conditions (Table 5).

Regarding the bimolecular toluene formation, a direct relationship between microporous volume and initial toluene

Table 5
Catalytic performance of six different zeolites: ethyltoluene conversion and molar selectivity

	ET X%	C2 S%	B S%	Tol S%	Xil. S%	EB S%	A_{10}^{+} S%
Beta	89.3	20.8	6.8	23.2	16.0	7.2	8.4
Mordenite	74.2	20.4	4.0	26.5	13.5	10.5	14.0
ITQ-23	94.7	31.7	10.0	22.4	14.7	4.3	3.6
NU-87	53.4	27.2	2.9	28.7	11.7	10.1	13.5
ZSM-5	95.6	41.8	6.7	36.3	7.8	1.3	1.4

Reaction conditions: 25 bar, 400 °C, WHSV 8 h^{-1}, and H_2/ET 8.5, TOS ~ 7 h.

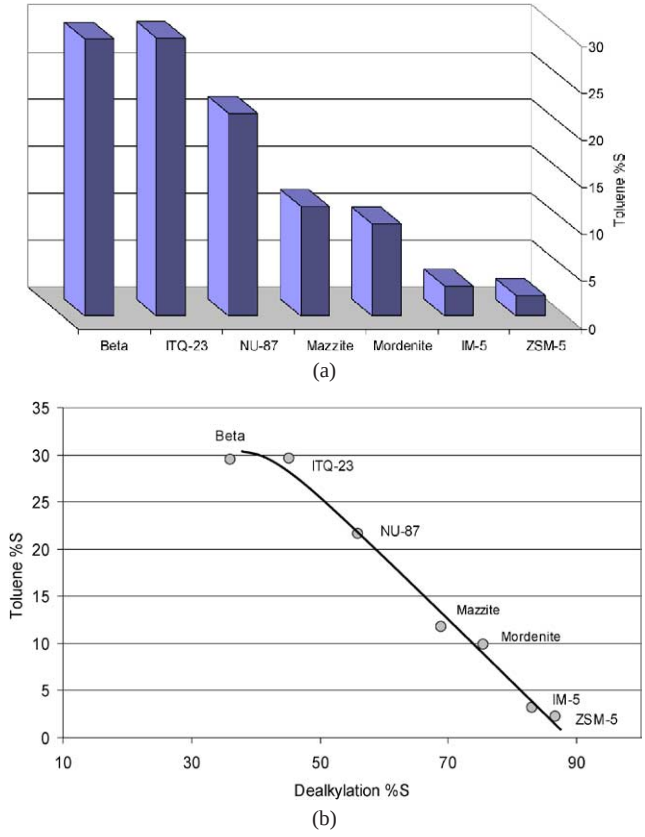

Fig. 5. Influence of zeolite structure in toluene and dealkylation selectivity. (Reaction conditions 25 bar, 400 °C, WHSV 8 h^{-1}, and H_2/EB 8.5, TOS ~ 8 h.)

selectivity can be seen, in such a way that the higher the pore size the higher the toluene selectivity (Fig. 5). More specifically, three types of behavior can be distinguished considering toluene selectivity: (1) 10-MR zeolites show a very

Table 6
Initial selectivities for five different zeolites

	EB X%	Dealkylation	Transalkylation	$C_3 + C_4$	Toluene	ET	Xylenes	Methane
Beta	2.6	0.0	95.5	0.0	4.5	4.4	0.0	0.0
NU-87	5.4	30.1	63.4	3.5	1.6	1.0	0.0	0.0
Mordenite	6.3	24.0	70.5	2.4	1.7	1.5	0.0	0.0
IM-5	6.1	51.6	45.9	0.0	1.2	0.8	0.0	0.0
ZSM-5	6.4	50.0	47.0	0.8	1.1	0.9	0.0	0.0

Reaction conditions: 25 bar, 400 °C, WHSV = 1400 h^{-1}, and H_2/EB ratio 8.5, TOS ~ 8 h.

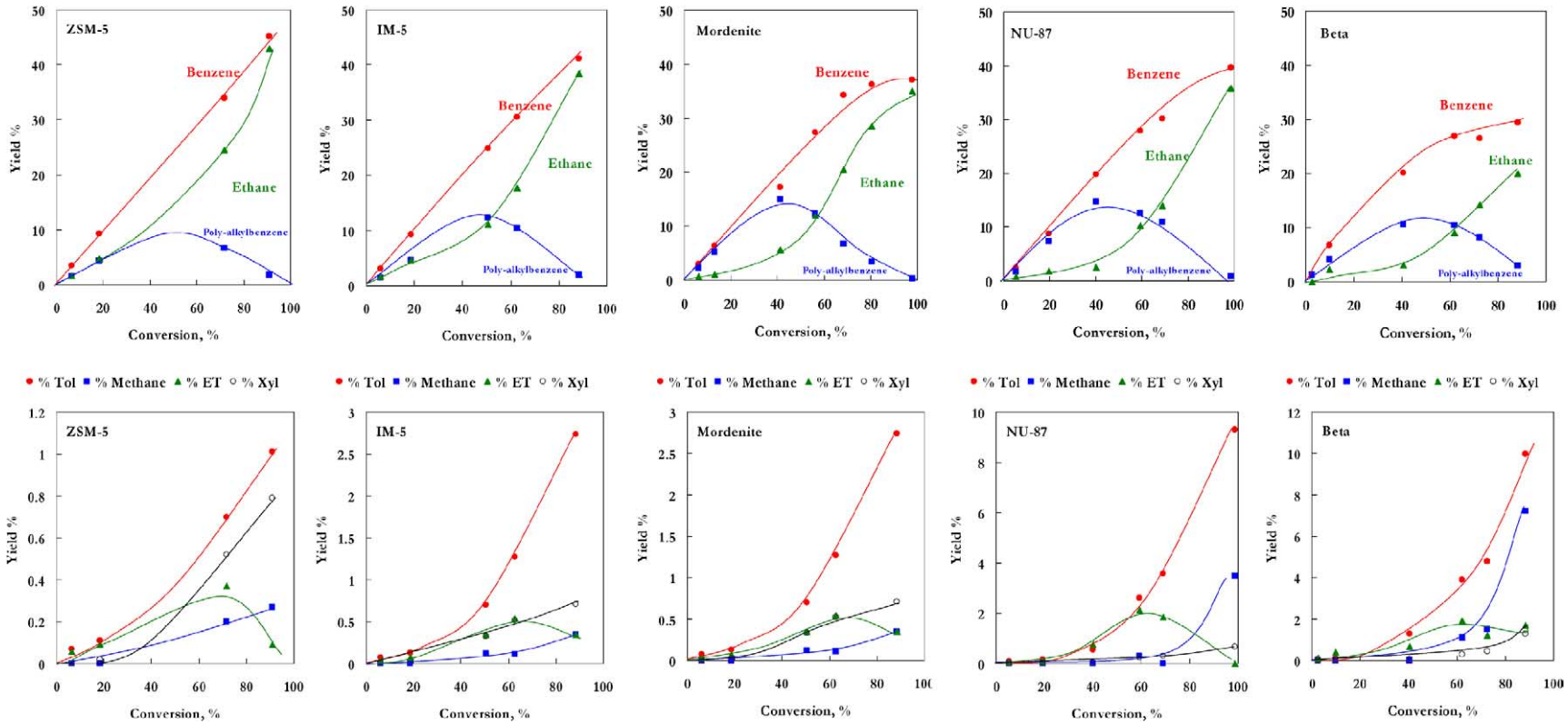

Fig. 6. Evolution of molar product yield with the EB conversion for five different zeolites. (Reaction conditions: 25 bar, 400 °C, WHSV 4 to 1400 h^{-1}, and H_2/EB 8.5, TOS ~ 8 h.)

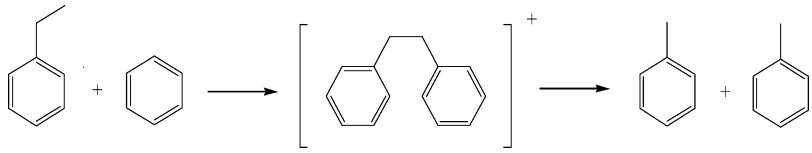

Scheme 7.

low (< 3%) toluene selectivity, (2) monodimensional 12-MR zeolites show a medium-low selectivity (5–10%) and (3) tridimensional 12-MR and 10-MR + 12-MR zeolites show a relatively high selectivity going from 20% for NU-87 to 28% for ITQ-23. The highest toluene selectivity is obtained over ITQ-23 zeolite, which contains the largest intrazeolitic cavity of all tested zeolites, although the cage windows are smaller than those contained in beta zeolite. Therefore, beta and ITQ-23 zeolite may have adequate cage geometries and sizes in order to allow the formation and stabilization of toluene-driving biphenylic intermediates. We can conclude that toluene formation is principally determined by zeolite structure, as can be concluded from the initial selectivities obtained at very short contact times (Table 6, WHSV 1400 h^{-1}). For all zeolites, toluene and ethyltoluene are formed in similar concentrations as primary reaction products whereas methane formation is not observed, confirming again that toluene is indeed formed via a bimolecular mechanism. The selectivity of five selected zeolites can be observed in Fig. 6, where the molar yields for major and minor reaction products versus EB conversion have been plotted. All zeolites show the same evolution for major reaction products as those observed for the reference catalysts (Fig. 2): in the early reaction steps the main reaction is the transalkylation of the ethyl group yielding poly-alkyl-aromatics that are progressively dealkylated. In all cases, a maximum in the poly-alkyl-aromatics yield is reached, and the value of this maximum depends on the zeolite structure.

Results from Fig. 6 show the effect of zeolite structure on toluene yield, being four times higher for beta and NU-87 than for IM-5 and mordenite. At low EB conversions, toluene and ethyltoluene are formed in equal amounts and very rapidly the yield of ethyltoluene starts to decrease. Toluene yield increases linearly when increasing conversions until ∼ 50% conversion, and then grows exponentially. The exponential increase in yield can be explained considering the two following contributions: (i) secondary conversion of ethyltoluene to produce ethane and toluene and (ii) transalkylation of EB and benzene to form two toluene molecules. The second reaction (Scheme 7) is specially favored at high EB conversions when benzene and EB are present at high concentrations. This reaction should also have a higher rate than other transalkylation reactions since diffusion of reactants and products is faster, and the lower size of the biphenylic intermediate allows a better stabilization inside zeolite cages, reducing the activation energy of the reaction.

4. Conclusions

During transalkylation of streams containing ethyl groups like heavy reformate, ethyl transalkylation reactions giving undesired poly-alkyl-aromatics occur at early reaction steps. An optimized catalyst should have a very active dealkylation function in order to minimize the formation of bulky poly-alkyl-aromatics that produce the progressive catalyst deactivation by coking and reducing the diffusion rate of reactants, like toluene or trimethylbenzene.

Ethylbenzene undergoes different bimolecular reactions giving as primary products either benzene and diethylbenzene or toluene and ethyltoluene, each reaction involving a different biphenylic intermediate (Scheme 4). The selectivity toward toluene formation is directly influenced by the zeolite pore size and geometry, with the highest toluene yield obtained with beta and ITQ-23. Catalytic results evidence that toluene formation from EB is a primary product that can be attributed to a bimolecular mechanism and not to the monomolecular hydrogenolysis of the terminal EB methyl group.

Zeolite pore structure has a direct influence on the ethyl dealkylation activity. The EB dealkylation selectivity strongly increases when decreasing the zeolite pore volume. Moreover, Re/IM-5 and specially, Re/ZSM-5 zeolites show an excellent dealkylation activity, allowing total and selective conversion of ethylbenzene into benzene and ethane under industrially practiced transalkylation reaction conditions. From our results, it appears that NU-87 and mordenite would be the preferred zeolites, since they combine at a good level dealkylation and transalkylation activities.

Acknowledgments

The author thanks the Institut Français du Pétrole and Comisión Interministerial de Ciencia y Tecnología (CICYT) (Project MAT 2003-07945-C02-01) for financial support.

References

[1] T.-C. Tsai, S.-B. Liu, I. Wang, Appl. Catal. A 181 (1999) 355.
[2] L. Mank, A. Hennico, J.L. Gendler, in: 20th 1995 Dewitt Petrochemical Review, 21–23 Marzo, 1995.
[3] T.C. Tsai, H.C. Hu, F.S. Jeng, K.Y. Tsai, Oil Gas J. 13 (1994) 115.
[4] S.H. Oh, S.I. Lee, K.H. Seong, Y.S. Seong, Y.S. Kim, J.H. Lee, in: Upgrading of Reformate and Heavy Aromatics to High-Value BTX, 2nd Asian Petrochem. Tech. Conference APTC 2002, 7–8 May 2002, Seoul, Korea, 2002.
[5] J.R. Mowry, in: R.A. Meyers (Ed.), Handbook of Petroleum Refining Processes, McGraw–Hill, New York, 1986, Sect. 10-10.

[6] Mobil Transplus Brochure, Mobil Technology Company.
[7] M. Guisnet, P. Magnoux, Appl. Catal. A 212 (2001) 83.
[8] K. Iwayama, R. Ichioka, H. Kato, H. Tanaka, US patent 6,359,184 (2002), to Toray Industries.
[9] M.D. Shanon, J.L. Casci, P.A. Cow, S.J. Andrews, Nature 353 (1991) 417.
[10] A. Corma, A. Chica, J.M. Guil, F.J. Llopis, G. Mabilon, A. Perdigón-Melón, S. Valencia, J. Catal. 189 (2000) 382.
[11] C.J. Kuei, L.J. Leu, Zeolites 9 (1989) 193.
[12] A. Corma, I. Giménez, S. Leiva, F. Rey, M.J. Sabater, G. Sastre, S. Valencia, in: Proceedings of 14th Int. Zeol. Conf., 25–30 April 2004, Cape Town, South Africa, 2004.
[13] J.H. De Boer, B.C. Lippens, B.G. Linsen, J.C.P. Broekhoff, A. van den Heavel, Th.V. Osinga, J. Colloid Interface Sci. 21 (1996) 405.
[14] C.A. Emeis, J. Catal. 141 (1993) 347.
[15] A. Corma, J.M. Serra, A. Chica, in: E.G. Derouane, V. Parmon, F. Lemos, F. Ramôa Ribeiro (Eds.), Principles and Methods for Accelerated Catalyst Design and Testing, Kluwer Academic, Dordrecht, 2002, p. 153.
[16] A. Corma, J. Hernández, J.M. Serra, (2001)World patent WO 0159463 (2001), to CSIC-UPV.
[17] H.G. Karge, J. Ladebeck, Stud. Surf. Sci. Catal. 5 (1980) 151.
[18] L.D. Fernandes, J.L.F. Monteiro, E.F. Sousa-Aguiar, A. Martinez, A. Corma, J. Catal. 177 (1998) 363.
[19] F. Alario, M. Guisnet, Catal. Sci. Ser. 3 (2002) 189.
[20] H.G. Karge, S. Ernst, M. Weihe, V. Weiss, J. Weitkamp, Stud. Surf. Sci. Catal. 84 (1994) 1050.
[21] J. Čejka, B. Wichterlová, Catal. Rev. 44 (2002) 375.
[22] G.A. Olah, A. Molnar, Hydrocarbon Chemistry, Wiley, New York, 1995.
[23] M. Guisnet, N.S. Gnep, S. Morin, Micropor. Mesopor. Mater. 35–36 (2000) 47.
[24] L.A. Clark, M. Sierka, J. Sauer, J. Am. Chem. Soc. 125 (2003) 2136.
[25] Y.S. Xiong, P.G. Rodewald, C.D. Chang, J. Am. Chem. Soc. 117 (1995) 9427.
[26] B. Wichterlová, J. Čejka, J. Catal. 146 (1994) 523.
[27] G. Mirth, J. Cejka, E. Nusterer, J.A. Lercher, Stud. Surf. Sci. Catal. 83 (1994) 287.
[28] N. Arsenova-Härtel, H. Bludau, W.O. Haag, H.G. Karge, Micropor. Mesopor. Mater. 35–36 (2000) 113.
[29] J.M. Silva, F. Ribeiro, M.R. Ramoa, E. Benazzi, M. Guisnet, Appl. Catal. A 125 (1995) 1–14.